EXPERIMENTAL SIMULATION OF REINFORCING BAR FRACTURE BY ASR

Yasushi Kawashima[1,*], Kenji Kosa[2], Hirotsugu Goda[2], Noriaki Koroki[2]

[1]Sumitomo Osaka Cement Co., Ltd. Cement-Concrete Laboratory
7-1-55, Minami-Okajima, Taisho-ku, OSAKA-City, Japan

[2]Kyushu Institute of Technology 1-1 Sensui, Tobata, KITAKYUSHU, Japan

Abstract

In this study, we investigated a 1/8th scale test set-up that simulated conditions for fracture of reinforcement bars by reproducing ASR expansion using expansive concrete inside a test specimen. We succeeded in reproducing brittle rupture in the bent sections of reinforcing bars. In addition, we identified the most important factors associated with rupture of reinforcing bars by investigating the crack depth and fracture surface of reinforcing bars.

Keywords: ASR, reinforcing bar rupture, knot shape, simulate, fracture surface

1 INTRODUCTION

The premature deterioration of concrete structures by alkali-silica reaction (ASR) is a major problem. In structures with significant ASR, bended parts and welded parts of the reinforcing bar have suffered rupture [1]. There is concern about the reduced load-carrying capacities of these structures, and consequently research has been conducted into elucidating the damage mechanisms of reinforcing bars.

In this study, experiments were performed to simulate AAR expansion and its effect on the rupture of reinforcing bars. This was done to clarify is an important factor in the rupture of reinforcing bars and to clarify the rupture mechanism of reinforcing bars. The most important factor to the rupture is clarified.

2 INVESTIGATIONS

A flow chart illustrating this study is shown in Fig. 1. The left side of Fig. 1 depicts the hypothesized reinforcing bar damage mechanism. It is conjectured that reinforcing bar rupture induced by ASR is caused by a combination of material degradation processes including initial cracking caused by bending, expansion of the concrete by ASR, and delayed fracture. In a previous study we found that the initial crack depth depends on the bending radius and the shape of knot of the reinforcing bar, and it was also clarified that a reinforcing bar became more susceptible to rupture with strain aging [2].

In this present study, reinforced concrete specimens were produced having various bending radiuses and knot shapes. The crack depths of the reinforcing bars were then measured, after applying pressure from inside the test specimens using expansive concrete. The principal causes and mechanisms of reinforcing bar rupture were examined by comparing the crack depth, before, during, and after expansion.

3 OUTLINE OF EXPERIMENT

3.1 Test specimen parameters

Parameters

The parameters of the test specimens used in this experiment are given in Table 1. The parameters investigated were bending radius, hoop ratio, type of reinforcing bar, and corrosiveness of the environment. The effect of the bending radius is compared in Cases 1~3, the effect of using a currently used reinforcing bars with the knot of old shape reinforcing bars (hereafter referred to as "old-type") is compared in Cases 4~6, and the effect of a corrosive environment is examined in Cases 6 and 8.

*Correspondence to: yakawashima@sits.soc.co.jp

Test specimen shapes and dimensions

The shapes and dimensions of the test specimens are shown in Fig. 2. The specimens used in this study consisted of an expansive concrete core surrounded by an outer layer of plain concrete. The purpose of this was to reproduce the internal expansion pressure that is generated by ASR. The dimensions of the test specimens were 1/8th those of actual bridge pier beams in which rupture of the reinforcing bar by ASR had been confirmed.

In the specimens, currently used D10 reinforcing bars form a hoop, one reinforcing bar was used in the cross-section so that it formed a square, while for the D16 reinforcing bars at the ends of test specimens, two reinforcing bars were joined so that they formed an L-shape imparting the double end with a hook like that shown in Fig. 2. This was because the length of the old-type D16 reinforcing bar was 1 m. The currently used D16 reinforcing bar was given a similar shape so that it could be compared with the old-type D16 reinforcing bar.

Manufacturing method and materials used

The mixtures for the plain and expansive concretes used to make the test specimens are given in Tables 2 and 3. The expansive concrete was poured into the internal cavity after the plain concrete had been wet-cured for two weeks. The mixture for the expansive concrete gave an expansion strain in excess of 1000×10^{-6}, which is a value thought that ASR damage is large. In addition, the mechanical properties and chemical composition of the reinforcing bars used in this experiment satisfied the values specified by the Japanese Industrial Standard (JIS G 3112).

The old-type reinforcing bar had a nitrogen content, which is readily affected by strain aging, that was almost equivalent to that of the currently used reinforcing bar, and there was no degradation in quality. In addition, in order to regard the effect of aging degradation on the reinforcing bars, they were heat-treated by placing them in an electric furnace at 120ºC for 10 hours. This heat treatment imparted strain aging that was equivalent to 6 years.

3.2 Measured parameters

Crack depth and knot shape

Observations of axial cross-sections were made in order to examine the initial crack depth in the bent sections of the reinforcing bars and to evaluate the progress of cracking and the knot shape of the reinforcing bars before bending. The method used for this is shown in Fig. 3, while the method used to measure the knot shape is shown in Fig. 4. The crack depths in the reinforcing bars were measured by taking half axial cross sections of the reinforcing bars in their bent sections and then observing these cross sections at a magnification of 50~200 under an optical microscope. In this examination, cracks found immediately after bending were classified as initial cracks and cracks observed after expansion pressure had been applied were classified as grown cracks. The knot shape measurement evaluated the diameter (φ) of the circle defined by the arc formed between the linear portion of the knot and the linear portion of the reinforcing bar (see Fig. 4).

Quantity of rust

In this experiment, the effect of a corrosive environment on damage to the reinforcing bars was examined. The circuit used to simulate a corrosive environment is shown in Fig. 5. A titanium mesh installed on the surface of the test specimen was used as the cathode, while the reinforcing bar was used as the anode; a currently used was made to flow between them. In order to induce corrosion in the reinforcing bar, the concrete was immersed in an electrolyte of an aqueous solution of NaCl (5%). In Case 6, the quantity of rust was estimated by finding 10% of the mass reduction rate of the reinforcing bar (i.e., there is a deficit at the whole circumference of reinforcing bar.), and in Case 8, it was estimated by finding 4.0% of the mass reduction rate (i.e., the condition that whole surface of the reinforcing bar product has corroded.) [3].

4 EXPERIMENTAL RESULTS

4.1 Comparison of largest crack damage

The effect of various factors on crack development was investigated by comparing the depth of the initial cracks that formed immediately after bending with the depth of mature cracks that developed after the application of expansion pressure. The maximum crack depths were compared in order to determine the conditions under which reinforcing bar rupture is most likely to occur.

The maximum crack depths of initial cracks and mature cracks are shown in Fig. 6. The maximum crack depth was made dimensionless by dividing it by the diameter of the reinforcing bar. Figure 6 shows that the crack depth around the expansion is large, when the bending radius is small in

the currently used D10 reinforcing bar. From this result, the size of the bending radius seems to promote the progress of the crack development. Crack growth in the old-type D16 reinforcing bar was dramatically greater than in the currently used D16 reinforcing bar; in particular, a maximum crack depth of 79.7% was observed. In the old-type reinforcing bar, the progress of crack development appears to be fast, since the cracks are large in the initial stages, as evidenced by the fact that large initial cracks were observed.

4.2 Effect of knot shape of the reinforcing bar

From the result of the preceding section, it is clear that the degree of crack development differs between the currently used D16 and old-type D16 reinforcing bars. The effect of different knot shapes on crack development could be quantitatively evaluated, since the material and machining conditions of the reinforcing bars did not appear to have a large effect on crack development.

The results of measuring the knot dimensions of all reinforcing bars are shown in Table 4. Table 4 shows that the knot interval of the reinforcing bars used and the knot height satisfy the permissible limit of JIS. However, it is important to measure the knot shape (φ), because regulations for the knot shape (φ) have not been established by JIS

The knot shapes of the three kinds of reinforcing bars are shown in Photo 1, and a comparison of the knot dimensions of all the reinforcing bars are shown in Fig. 7. The knot shape parameter measured was the diameter of the arc of three knots. The value obtained by dividing the mean value by the reinforcing bar diameter was then used to evaluate the knot shape.

In Fig. 7, the ratio of the φ to the diameter of the reinforcing bar (defined as a knot shape change rate) is 42% for the currently used D10, 44% for the currently used D16, and 7.0% for the old-type D16. Therefore, the knot geometries of old-type reinforcing bars and currently used reinforcing bars differ by a factor of over six times. Large cracks appear to develop more readily in the old-type reinforcing bars than in the currently used reinforcing bars, since in φ is small, large stress concentrations and plastic deformations are generated in the bent region, and, as a result, large cracks develop in the root of the knot.

4.3 Characteristics of crack growth

Figure 6 shows that a large crack developed in the old-type D16. The position where the crack developed most was examined, because multiple cracks are generated in one reinforcing bar by bending. Figure 8 shows a comparison of mature cracks in old-type reinforcing bars. In this figure, all mature cracks that formed in the bent sections of two old-type reinforcing bars embedded in one test specimen were compared. The reason why only one crack was measured for Cases 6-2 and 7-2 is because these specimens were used for observing the fracture surface. Figure 8 confirms the tendency for the particular crack depth to increase in bent sections. Based on this finding, the generation position of the largest mature crack was examined. This is because there seems to be an especially weak point in the bent section of a reinforcing bar.

Figure 9 shows the number of cracks generated at two different crack initiation positions. In Fig. 9, the knot that appears to be affected by bending is labeled in the following way: A: beginning section of bending, B: beginning and middle regions of bending, C: central region of bending. Figure 9 shows the locations of the largest cracks generated after the application of the expansion pressure; in five out of six cases these locations were in region C. In a previous study, three-dimensional FEM analysis of the strain generated in the bending of the reinforcing bar demonstrated that the plastic strain is concentrated near region C [1]. Our experimental results confirm that this region is a weak point, since we found a high concentration of large mature cracks in region C.

4.4 Effect of corrosion

Next, the effect of a corrosive environment was investigated. In this section, we consider the effect of corrosion and hydrogen embrittlement on ASR-induced damage to reinforcing bars. In this experiment, a corrosion test was performed to examine the effect of corrosion on crack growth in reinforcing bars. The corrosion loss measurement results are shown in Table 5; they are reasonably close to the desired values for this kind of test.

Next, a comparison experiment for mature crack damage was carried out. Table 6 shows the largest damage (in the 90° bent section) to the old-type D16 reinforcing bars for each case. The largest damage was 40.8% at a corrosion loss of 4.0% and 78.8% at a corrosion loss of 10%. However, the largest damage occurred in the case when there was no corrosion, in which 79.6% damage occurred. This confirms that equivalent damage was generated in the case of only expansion pressure.

The structures of two axial cross-sections of a reinforcing bar removed from a test specimen of the corrosion test are shown in Photo 2. Although pitting corrosion caused by corrosion was observed (Photo 2a), corrosion in the cracked part was not observed (Photo 2b). Thus, evidence that corrosion assisted crack development was not obtained. Based on the above results, it appears to be unlikely that corrosion is directly related to the development of cracks.

4.5 Results of the reinforcing bar fracture surface investigation

In this experiment, rupture of the reinforcing bar in Case 7 in the hoop bending section was observed on the sixth day after adding the expansive concrete. Figure 10 shows the rupture position of the reinforcing bar and a photograph of the rupture cross-section. The rupture location was in the vicinity of the hook at which the old-type reinforcing bar D16 was bent at an angle of 135° and had a bending radius of 1.00d. Corrosion was not observed on the fracture surface, and the rupture was caused by brittle fracture without elongation or restriction, and it agreed with the features of rupture of the reinforcing bar of the existing structure. Figure 11 shows scanning electron microscope images of the fracture surface of the reinforcing bar.

The fracture surface of the reinforcing bar is classified into the regions ① ~ ④ inside the bending sections. ① is a primary crack that appears to have been generated during bending. ② is a secondary crack in which a primary crack appears to develop by expansion pressure. The progress of the secondary crack seems to temporarily stop in region ③. ④ is a tertiary crack in which the rupture is generated. The observation results show region ① of the fracture surface, in which the ductile fracture surface occurred, and the aspect of the shear fracture surface. Both regions ② and ④ exhibited brittle fracture surfaces. Region ③ was the narrow and belt-like area at the boundary of regions ④ and ②. It has a dimple pattern, which is a characteristic of ductility fracture surfaces.

In the above results, the fracture surfaces in the bent sections of reinforcing bars obtained in this experiment had properties close to those of fracture surfaces in other structures, and to some extent it was possible to simulate actual damage.

5 DISCUSSION

5.1 The rupture mechanism of reinforcing bars

Figure 12 shows an overview of the rupture mechanism of reinforcing bars. The following are points are depicted. The rupture mechanism depicted is based on experimental results and it identifies the main processes. In the testing conditions for Case 7 it is possible to classify the factors responsible for rupture of the reinforcing bar into two categories: those that occur during construction and those that occur during application of expansion pressure (see Fig. 12). Processes that occur during construction are ① use of the old-type reinforcing bars and ② generation of large initial cracks during bending. Those that occur during application of expansion pressure are ③ generation cracks during strain aging and ④ development of cracks due to expansion pressure. It is considered that rupture of reinforcing bars occurs due to the combination of process during construction and process during crack growth.

6 CONCLUSIONS

(1) The use of old-type reinforcing bars seems to be a matter of great concern for rupture of steel reinforcing bars, because the occurrence of initial cracks and mature cracks in old-type reinforcing bars was much greater than in currently used reinforcing bars.

(2) Some cracks tend to develop in cracks in the bent section. The location where most cracks were initiated is knot C (located almost at the center of the bent section), in which cracks occurred in five out of six samples.

(3) There was no apparent difference between the damage in steel reinforcing bars in a corrosive environment and in a non-corrosive environment. There seems to be a low likelihood that a corrosive environment is directly related to crack development.

(4) Based on the experimental results, the following four factors are considered to be important in the rupture of reinforcing bars: 1) the use of old-type reinforcing bars having a knot shape change rate of 10%, 2) the generation of initial cracks during bending, 3) embrittlement caused by strain aging, and 4) the development of cracks by the application of expansion pressure.

7 REFERENCES

[1] Japan Society of Civil Engineers : Concrete Library No.124, State-of-the Art Report on the Countermeasures for the Damage Due to Alkali-Silica-Reaction, 2005.

[2] K.Kosa, Y.Kawashima, Y.Shinno, K.Sasaki,: The Material Testing for Reinforcing Steel Rupture Mechanism Estimation by Alkali-Aggregate Reaction, Journal of Structural Engineering, 2006.3 (52A): 951-958 (in Japanese).

[3] S.Tottori, Y.kamino, M.Kitago, T.miyagawa, Durability Evaluation of Existing Railway Viaduct from the Viewpoint of Corrosion of Steel, The Symposium Proceedings on the Rehabilitation of the Concrete Structure, (1998.10): 49-54.

TABLE 1 : The test specimen parameters.

Type of specimen	Bending radius [1)]	Hoop ratio (%)	Type of reinforcing bars [2)]	Corrosion environment
Case 1	1.0d	0.147	Current D10	Not consideration
Case 2	1.25d			
Case 3	0.75d			
Case 4	1.0d	0.410	Current D10 Current D16	Not consideration
Case 5				
Case 6			Old-type D16	10% corrosion loss
Case 7			Current D10	Not consideration
Case 8			Old-type D16	4% corrosion loss

1) d : Diameter of reinforcing bar, 2) D : Deformed reinforcing bar

TABLE 2 : Mix propotions for the plain. concrete

Gmax (mm)	W/C (%)	s/a (%)	Unit quantity (kg/m^3)				Admixture (kg/m^3)
			W	C	S	G	
20	46	43	175	381	718	1018	1.142

TABLE 3 : Mix propotions for the expansive. concrete

W/C (%)	Unit quantity (kg/m^3)				
	W	C	S	G	Expansive admixture
40	230	575	1150	0	200

TABLE 4 : Measurement results of the knots.

Type of reinforcing bar		Average knot interval	Average knot height	Knot shape(ϕ)
Current D10		6.5 mm	0.51 mm	4.2 mm
Current D16		8.2 mm	0.83 mm	7.1 mm
Old-type D16		10.1 mm	1.12 mm	1.1 mm
Allowable limit	D10	3.7 mm(max)	0.4～0.8 mm	—
	D16	11.1 mm (max)	0.7～1.4 mm	—

TABLE 5 : Average corrosion loss.

Case 6 Desired value 10%	Average corrosion loss	Case 8 Desired value 4%	Average corrosion loss
Current D10	13.4%	Current D10	5.5%
Old-type D16	10.7%	Old-type D16	2.9%
Current D16	7.9%	Current D16	—

TABLE 6 : Crack damage in the old-type D16.

Set value of corrosion loss (%)	Maximum crack depth / Diameter (%) Old-type D16 Largest Damage		
0.0	4.8	31.9	79.6
4.0	40.8	—	—
10.0	78.8	—	—

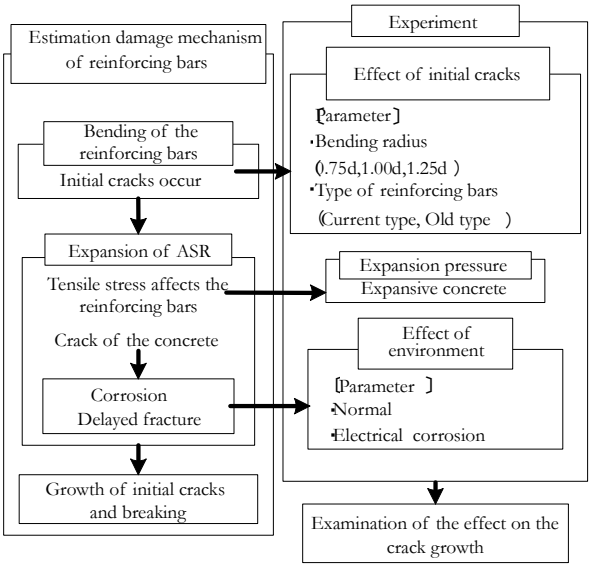

Figure 1 : Flow chart describing this study.

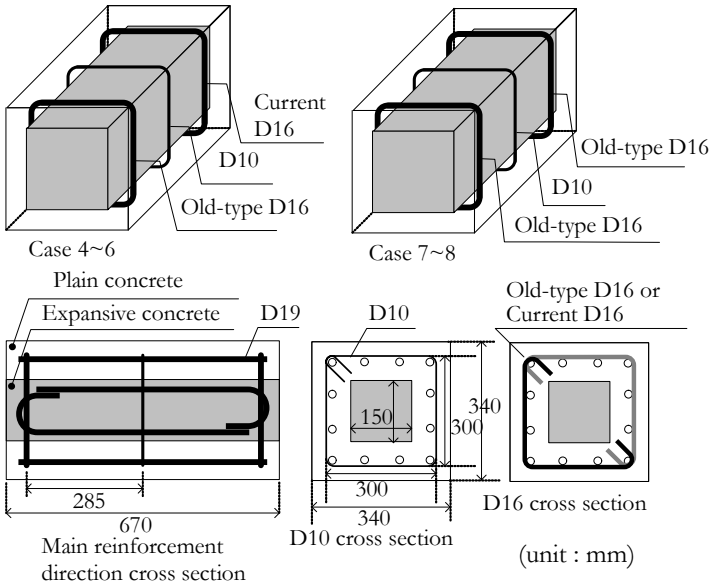

Figure 2 : Shape and dimensions of test specimens.

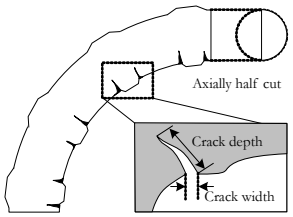

Figure 3 : Method for measuring cracks.

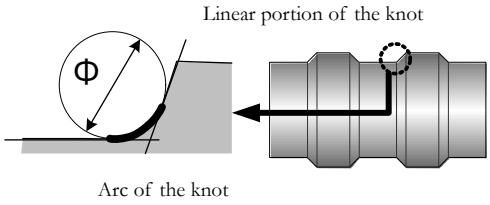

Figure 4 : Method for measuring knot shape.

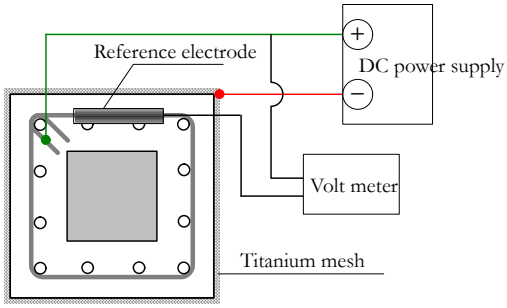

Type of specimen	Electric Amperes	Time Hours	Water solution NaCl
Case 6	0.15	504	5.00%
Case 8		197	

Figure 5 : Circuit and electrical parameters.

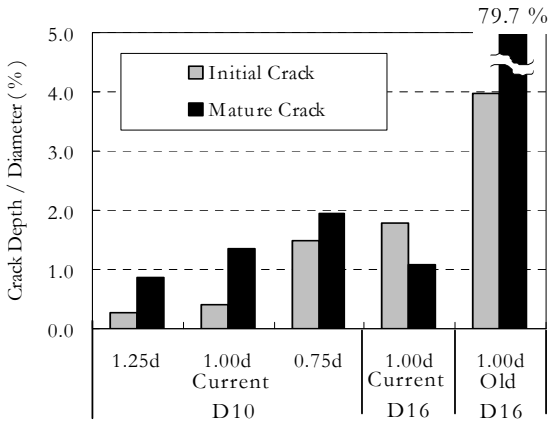

Figure 6 : Comparison of the maximum crack depths.

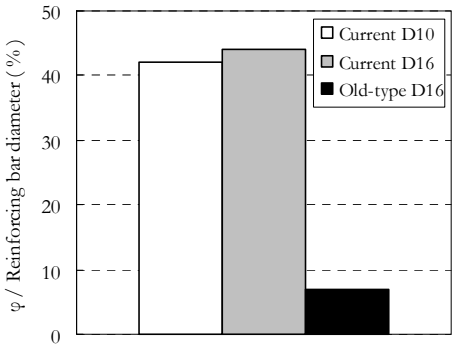

Figure 7 : Comparison of the knot shapes.

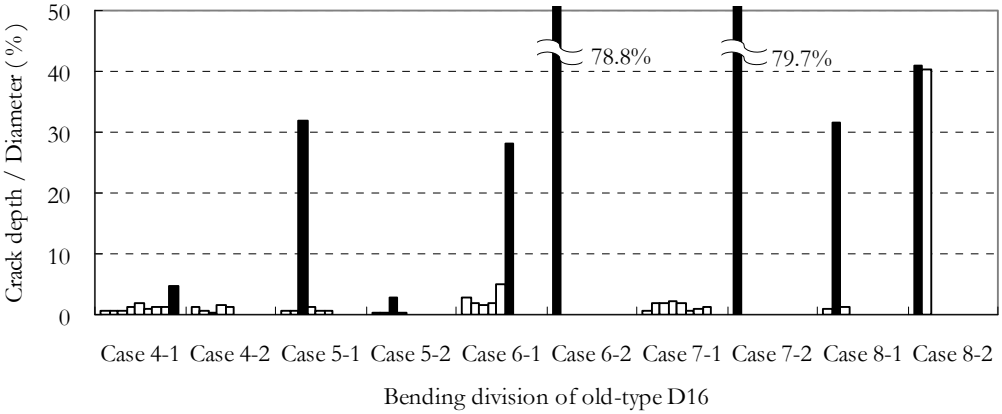

Figure 8 : Comparison of depth of mature cracks in old-type reinforcing bar.

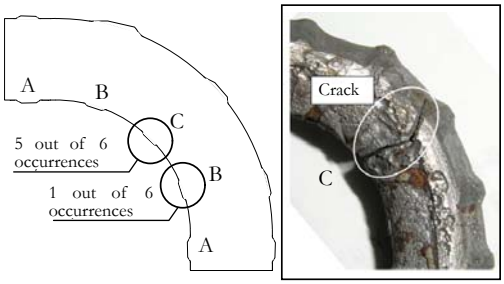

Figure 9 : Position of Cracks.

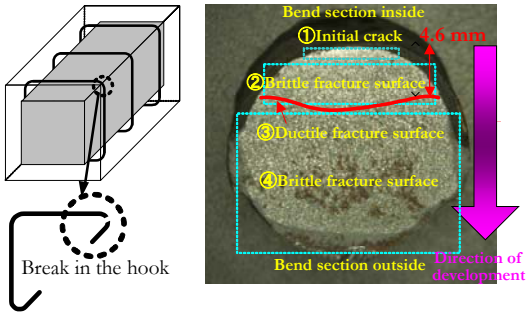

Figure 10 : Rupture of a reinforcing bar.

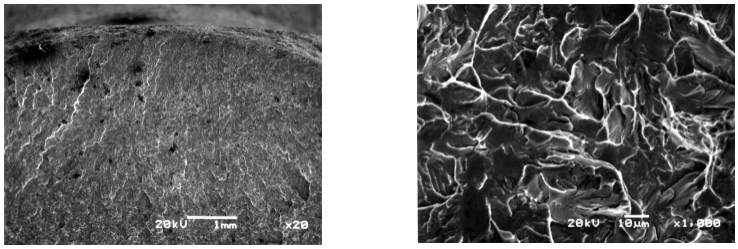

①Ductility fracture surface　②Brittle fracture surface

③Ductility fracture surface　④Brittle fracture surface

Figure 11 : SEM observation results of the fracture surface of a reinforcing bar.

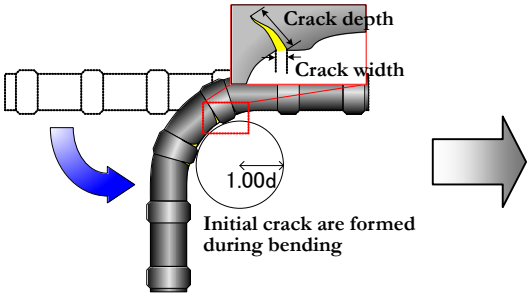

Process during construction

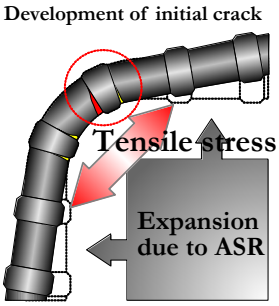

Process during crack growth

①Use of the old-type reinforcing bar
φ of current reinforcing bars is over 6 times of the old-type reinforcing bars

②Generation of large initial cracks during bending
Current: 0.62% (Average)
Old-type: 1.43% (Average)
2.3times

③Embrittlement phenomenon due to strain aging
Strain aging that corresponds in 6 years

④Development of cracks by application of expansion pressure
Current: 0.8% (Average)
Old-type: 1.43% (Average)
79.7% (Maximum)
7.2times

Figure 12 : Rupture mechanism of reinforcing bar.

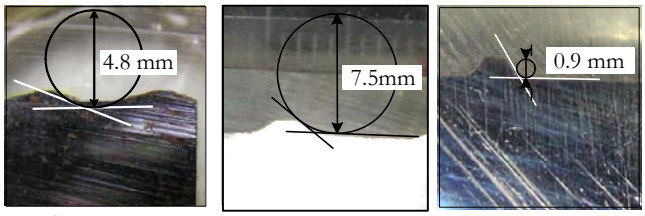

Current D10　Current D16　Old-type D16

Photo 1 : Knot shapes.

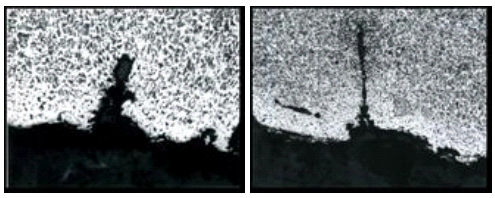

a) Pitting corrosion b) Crack

Photo 2 : Structure of axially cross sections.